REVIEW

Spectrum of Magnetic Resonance Imaging Findings in Pancreatic and Other Abdominal Manifestations of Von Hippel-Lindau Disease in a Series of 23 patients: A Pictorial Review

Rossella Graziani[1], Simona Mautone[2], Mario Vigo[1], Riccardo Manfredi[2], Giuseppe Opocher[4], Massimo Falconi[3]

[1]Department of Radiology, Abano Terme Hospital. Abano Terme (PD), Italy.
Departments of [2]Radiology and [3]Surgery, University of Verona, "G.B. Rossi" Hospital. Verona, Italy.
[3]Department of Oncology, Veneto Institute of Oncology. Padua, Italy

ABSTRACT

Context Von Hippel Lindau disease is a rare autosomal dominantly inherited multisystem disorder characterized by development of benign and malignant tumors. The abdominal manifestation of the syndrome are protean. Magnetic resonance plays an important role in identification of abdominal abnormalities and follow-up of lesions. **Objective** To describe magnetic resonance imaging findings and patterns of pancreatic and other principal abdominal manifestations in a series of von Hippel-Lindau (VHL) disease patients and to review literature. **Methods** We retrospectively reviewed abdominal magnetic resonance studies performed in 23 patients (10 males, 13 females) diagnosed of VHL. **Results** In all examined patients abdominal involvement was present. The pancreatic imaging findings detected were: unilocular cystic lesions (6/23: 26.1%); serous cystadenomas (11/23: 47.8%), including diffuse lesions (8/23: 34.8%); solid neuroendocrine tumors (8/23: 34.8%); cystic neuroendocrine tumors (1/23: 4.3%). The renal findings detected were: simple renal cysts (18/23: 78.3%); complex renal cysts (13/23: 56.5%), including benign lesions (10/23: 43.5%) and malignant lesions (3/23: 13.0%); renal carcinomas (11/23: 47.8%) and 5 of these (45.5%) were multiple and bilateral. Five patients (21.7%) presented pheochromocytoma (4 of these were bilateral; 80.0%) and 1 patient (4.3%) presented cystadenoma of the epididymis. **Conclusions** In VHL disease patients, magnetic resonance imaging plays an essential role in the identification of pancreatic and other abdominal lesions, in their follow-up, in the screening of asymptomatic gene carriers, and in their long-term surveillance.

INTRODUCTION

Von Hippel-Lindau (VHL) disease is a rare, autosomal dominantly inherited multisystem disorder with a 50% chance of inheriting the VHL gene from a carrier [1]. The prevalence is estimated to be between 1 in 31,000 and 1 in 53,000 [1, 2, 3, 4].

It is associated with inactivation of a tumor suppression gene located on chromosome 3p25.5 [5, 6, 7, 8, 9, 10].

The gene has high penetrance but variable expression, resulting in a wide variety of manifestations of the disease in affected individuals. The spectrum of most frequent clinical manifestations of the disease includes retinal and central nervous system hemangioblastomas, endolymphatic sac tumors, and multiple abdominal lesions: renal cysts and tumors, pancreatic cystic lesions (simple cysts, serous microcystic or micro/macro-cystic cystadenoma), pancreatic solid lesions, the most common neuroendocrine tumors (NETs), frequently non-functioning, pheochromo-cytomas, and epididymal cystadenomas.

According to the natural history of the disease, the median life expectancy is 49 years [4, 11]. Thanks to recent diagnostic imaging modalities, clinical screening and advanced surgical techniques, the morbidity and mortality of patients with VHL disease has been reduced significantly over the past 20 years [4, 11].

The diagnostic criteria for VHL disease [12] include the following: a) more than one central nervous system hemangioblastoma; b) one central nervous system hemangioblastoma and visceral manifestations of VHL disease; and c) any manifestation and a known family history of VHL disease.

The abdominal manifestations of VHL tend to be asymptomatic at the onset of the disease and they are frequently diagnosed later than other manifestations.

Patients with VHL disease require long-term follow-up of abdominal manifestations with imaging techniques. Magnetic resonance (MR) is imaging method of choice for follow-up, because of the absence of radiation. Several authors suggest annual surveillance of abdominal manifestations with MR imaging [12, 13, 14, 15, 16].

The aim of this paper is to focus on principal MR imaging findings of pancreatic and other principal abdominal manifestations of VHL disease patients we have been observed and to review the literature.

MATHERIAL AND METHODS

Patients Population

A search in medical and surgical records and radiological database of two different institutions (Abano Terme Hospital and University Hospital of Verona) between January 2007 and January 2011, disclosed 72 patients suffering from VHL syndrome to be considered for the inclusion in this retrospective study.

Inclusion criteria were VHL syndrome confirmed by genetic tests, imaging examination (64-slice multidetector CT (MDCT)) scanning and/or 1.5 T magnetic resonance (MR) scanning) performed at moment of diagnosis, availability of surgical specimens, and histopathological examination of the VHL cases submitted to surgical procedure.

Exclusion criteria were imaging (MDCT and/or MR) not performed at the moment of diagnosis (30 patients), patients studied only with MDCT technique (2 patients), unavailability or poor quality of imaging (7 patients), lack of surgical procedure (5 patients), and specimen not available (5 patients) in VHL cases submitted to surgical procedure.

We retrospectively evaluated 23 patients (10 males, 13 females) with mean age of 45 years (range: 24-69 years), who underwent abdominal MR imaging at the clinical onset and diagnosis of the disease. Seven patients (30.4%) were family members (3 different families).

At diagnosis 10 patients were asymptomatic (43.5%). In the remaining 13 symptomatic patients, referred symptoms were: pancreatic pain (9, 69.2%), acute pancreatitis episodes (4, 30.8%), biliary obstruction (5, 38.5%), exocrine pancreatic insufficiency (6, 46.2%), hypertension (5, 38.5%), palpitations and sweating (4, 30.8%). All patients presented more than one symptom. Pathological specimen was performed after pancreatic surgical procedures in 13 patients (56.5%; 4 pancreatico-duodenectomies with Whipple procedure, 4 distal splenopancreatectomies, 3 total pancreatectomies; 1 cystojejunoanastomosis, 1 enucleation), after renal surgery in 14 (60.9%; 6 nephrectomies, 8 simple enucleations of the mass or partial nephrectomy). Out of these, multiple (pancreatic and renal) different surgical procedures were performed in the same patient in 5 cases (in 2 cases splenopancreatectomy and nephrectomy; in 1 case pancreaticoduodenectomy and partial nephrectomy; in 1 case cystojejunoanastomosis and partial nephrectomy; in 1 case pancreatic enucleation and partial nephrectomy). In addition, surrenectomy was made in 5 cases (38.5%; 4 were bilateral) and testicular resection in 1 case.

Imaging Technique

MR imaging was performed at 1.5 T scanner (Achieva, Philips, Heindoven, Holland; Magnetom Symphony, Siemens, Erlangen, Germany), using 16 and 4 channel phased array coil, respectively.

The patients were asked to fast 4-6 hours before the examination. Furthermore, to eliminate overlapping fluid-containing organs on T2-weighted images, 50-150 mL of superparamagnetic iron oxide particles (ferumoxsil, Lumirem, Guerbet, Aulnay-sous-Bois, France) were administered 10-20 minutes before MR imaging. The MR imaging protocol and pulse sequence parameters are reported in Table 1. The dynamic study, during gadolinium-chelates injection, was obtained by means of T1-weighted gradient echo 3D volumetric pulse sequence using

Table 1. Magnetic resonance imaging protocol: pulse sequences and parameters.

Pulse sequence	Plane	Repetition time (msec)	Echo time (msec)	Slice thickness (mm)
Chemical shift T1-weighted gradient echo	Axial	107-160	2.4-4.8	7-8
Fat-saturated T2-weighted (RARE)	Axial	4,000-4,950	91-102	7-8
T2-weighted half Fourier RARE (HASTE)	Coronal and axial	∞	60-102	4-6
T2-weighted half Fourier RARE (HASTE)	Coronal	∞	102-400	40-60
2D half Fourier RARE (HASTE) MRCP	Multiple	∞	1100	40-80
Fat-saturated 3D volumetric gradient echo (VIBE)	Axial	4.66	1.87	2.6-3

2D: two dimensional; 3D: three dimensional; HASTE: half Fourier single-shot turbo spin-echo; MRCP: magnetic resonance cholangiopancreatography; RARE: rapid acquisition with relaxation enhancement; VIBE: volumetric interpolated breath-hold examination

parallel imaging. A quadriphasic dynamic study was performed during 0.1 mmol/kg body weight gadolinium-chelates injection (Multihance, Bracco, Milan, Italy or Dotarem, Guerbet, Aulnay-sous-Bois, France) by means of a power injector (Spectris, Medrad, Pittsburgh, PA, USA) at 2-2.5 mL/sec, by acquiring the pre-contrast phase, late arterial/pancreatic phase (scan delay: 35-45 sec), portal venous phase (scan delay: 75-80 sec), and delayed phase (scan delay greater than 180 sec).

Image Analysis

MR images were retrospectively evaluated by two readers in consensus (R.G., S.M.). The retrospective reviewers were blinded to the presence of abdominal lesions of VHL disease, but they were not blinded to the type and abdominal site of lesions. All MR images were assessed at the workstation.

In qualitative analysis about pancreas we evaluated: unilocular fluid lesion or simple cystic lesion; serous micro- or micro/macro-cystic cystadenoma; hypervascular solid lesion or hypervascular non functioning NET; cystic lesion with thickened enhanced walls or cystic non-functioning NET; association of non-functioning NET and cystic lesion (serous cystadenoma, simple cystic lesion); vascular invasion; retroperitoneal lymph nodes; liver metastasis (about all of them: presence/absence and site of pancreatic lesion: head, body-tail or diffuse in all pancreatic gland). About kidney we evaluated: fluid lesion or cyst; fluid and solid lesion or complex cyst; completely solid lesion or tumor, hypervascular during contrastographic arterial phase with wash-out during portal venous phase; renal vascular invasion; retroperitoneal lymph nodes; liver metastasis (about all of them: presence/absence; unilateral/bilateral lesions; unique lesion/multiple lesions).

About adrenal gland we evaluated: solid hyper-vascular tumor (presence/absence; unilateral/bilateral lesions).

About scrotum were evaluated: cystic lesion; solid lesion (presence/absence; unilateral/bilateral lesions).

In quantitative analysis major diameter of single lesion, or major diameter of major lesion in case of multiple lesions, were measured.

STATISTICS

Mean and range, as well as absolute and relative frequencies were used as descriptive statistics. Interobserver variability was analyzed with the kappa statistic. Results of interobserver agreement were classified as 0.20 slight, 0.21-0.40 fair, 0.41-0.60 moderate, 0.61-0.80 substantial and 0.81-1.00 almost perfect.

RESULTS

Thirty-four pancreatic lesions were found in the 23 patients. In qualitative analysis, the MR imaging findings were: 6 (26.1%) unilocular fluid cystic lesions (Figure 1abc): 3 (13.0%) in pancreatic head, 3 (13.0%) in pancreatic body-tail; 11 (47.8%) serous micro- or micro/macro-cystic cystadenomas (Figures 1def, 4, and 5): 1 (4.3%) in pancreatic head, 2 (8.7%) in pancreatic body-tail (Figure 1), 8 (34.8%) diffuse (Figures 4 and 5); 8 (34.8%) neuroendocrine solid tumors: all of them non-functioning NET and hypervascular during arterial pancreatic phase of contrastographic dynamic study (Figures 2, 3, 4, and 5), 4 (17.4%) at pancreatic head (Figures 2ab; 3ace, and 4), 4 (17.4%) at pancreatic body-tail (Figures 2cd and 5); 1 (4.3%) cystic non-functioning NET, diffuse in all pancreatic gland (Figure 6); in 4 (17.4%) cases association of non-functioning NET and pancreatic cystic lesions (3 cases of association of non-functioning NET and serous cystadenoma (13.0%); 1 case of association of non-functioning NET and pancreatic simple cystic lesion (4.3%)) were present (Figures 4 and 5). Vascular invasion was not detected in any patients.

The 42 renal MR imaging findings present in qualitative analysis were: 18 (78.3%) renal cysts: 16 (69.6%) bilateral and multiple and 2 (8.7%) single (Figures 2d, 4ab, 5adef, and 7abcdef); 13 (56.5%) complex renal cysts: including 10 (43.5%) benign complex renal cysts (Figures 1a and 2b) and 3 (13.0%) malignant or cystic renal carcinoma (Figures 4ef and 7bcdef); 11 (47.8%) solid renal carcinomas hypervascular during arterial phase of contrastographic study with wash-out during portal venous phase: 5 (21.7%) multiple and bilateral and 6 (26.1%) single. Only 1 of these 11 lesions at pathological specimen resulted benign or adenoma.

The adrenal MR imaging findings were: 5 (21.7%) solid hypervascular tumors, 4 (17.4%) bilateral and 1 (4.2%) monolateral (Figure 8abcd).

The scrotum MR imaging findings were: 1 (4.3%) fluid cystic lesion or cystadenoma (Figure 9) and none solid lesion.

Vascular invasion was not detected in any patients. In 2 cases (8.7%) retroperitoneal lymph nodes, both of them in neuroendocrine tumors, were present. Liver metastasis were detected in none.

Interobserver variability showed almost perfect agreement for the following pancreatic parameters: i) presence/absence; ii) site of pancreatic lesions in pancreatic head, iii) lesions in body-tail; and iv) lesions diffuse in all pancreatic gland. The kappa values of unilocular fluid cystic lesions were: 0.895, 0.888, 0.943, and 0.966, respectively; those of serous cystadenomas were 1.000, 0.972, 0.999, and
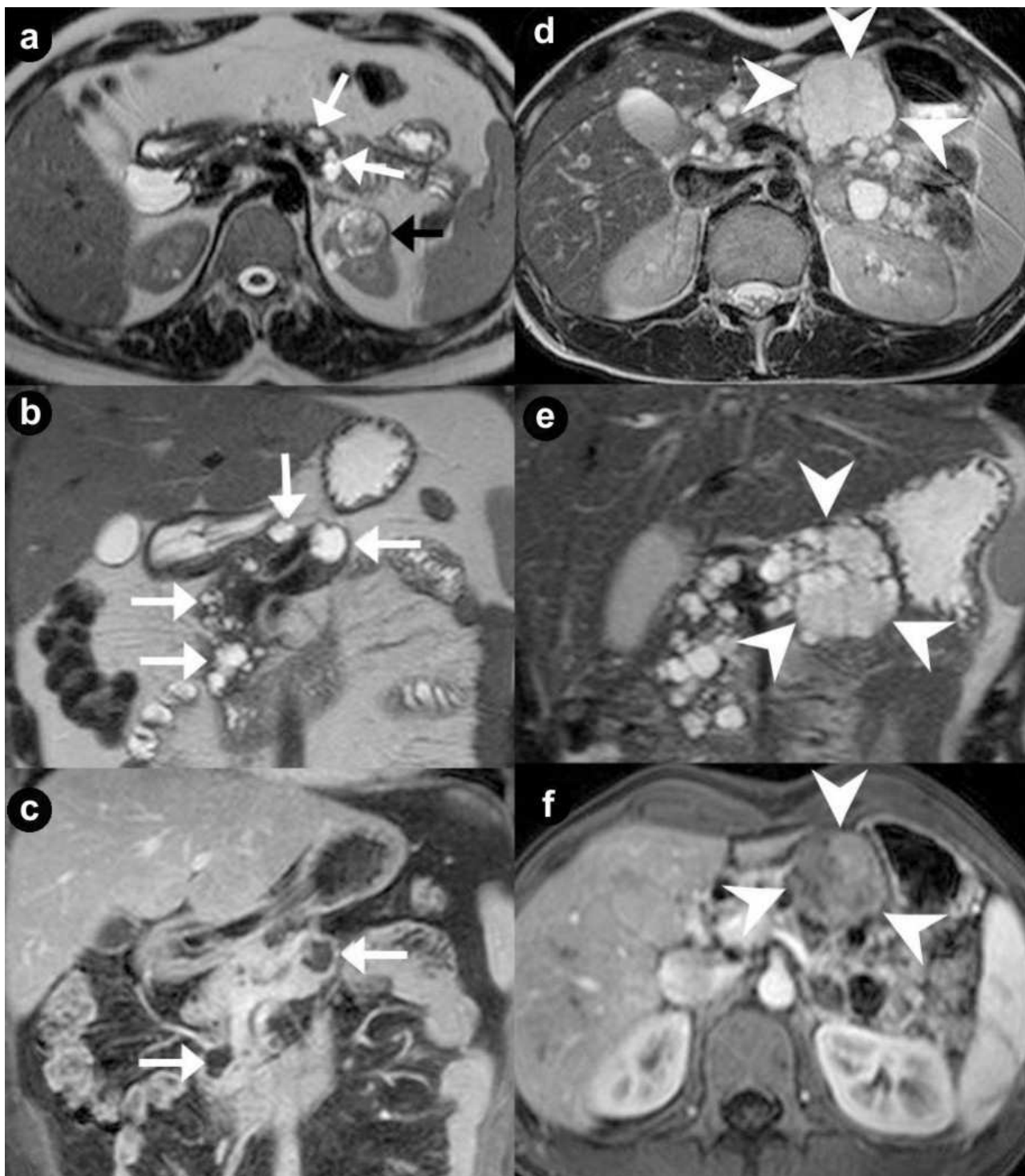
Figure 1. Pancreatic unilocular cysts (**a. b. c.** Case#1: 35-year-old man with VHL disease). Pancreatic microcystic serous cystadenoma (**d. e. f.** Case#2: 30-year-old man with VHL disease). Axial (**a. d.**) and coronal (**b. e.**) T2-weighted MR images; coronal (**c.**) and axial (**f.**) 3D volumetric gradient-echo T1-weighted fat suppressed images after intravenous contrast medium administration during arterial pancreatic phase of contrastographic dynamic study.

Case#1. Multiple fluid, cystic lesions of pancreatic parenchyma with different size and site (arrows), hyperintense on T2-weighted MR images, are present (**a. b. c.**). Cystic lesions do not communicate with the main pancreatic duct, which appears not dilated. The cystic walls do not show enhancement after intravenous contrast medium administration (**c.**). In the upper pole of the left kidney (**a.**) a complex cystic mass (black arrow) is detected.

Case#2. A lobulated fluid mass, with thin walls, hyperintense at T2-weighted images (**d. e.**), is present in the body of pancreatic gland (arrowheads). Inside the mass, containing multiple fluid cystic areas, multiple radially aligned thin septa are visible (spongy appearance or honeycomb pattern). The septa and the peripheral walls enhance after intravenous gadolinium administration (**f.**). The septa are well depicted on coronal T2-weighted MR image (**e.**) but the central scar is not visible. In the remaining portion of pancreatic gland multiple cystic, fluid, round lesions, with different size and site and without enhancement after intravenous contrast medium administration (**f.**), are present.
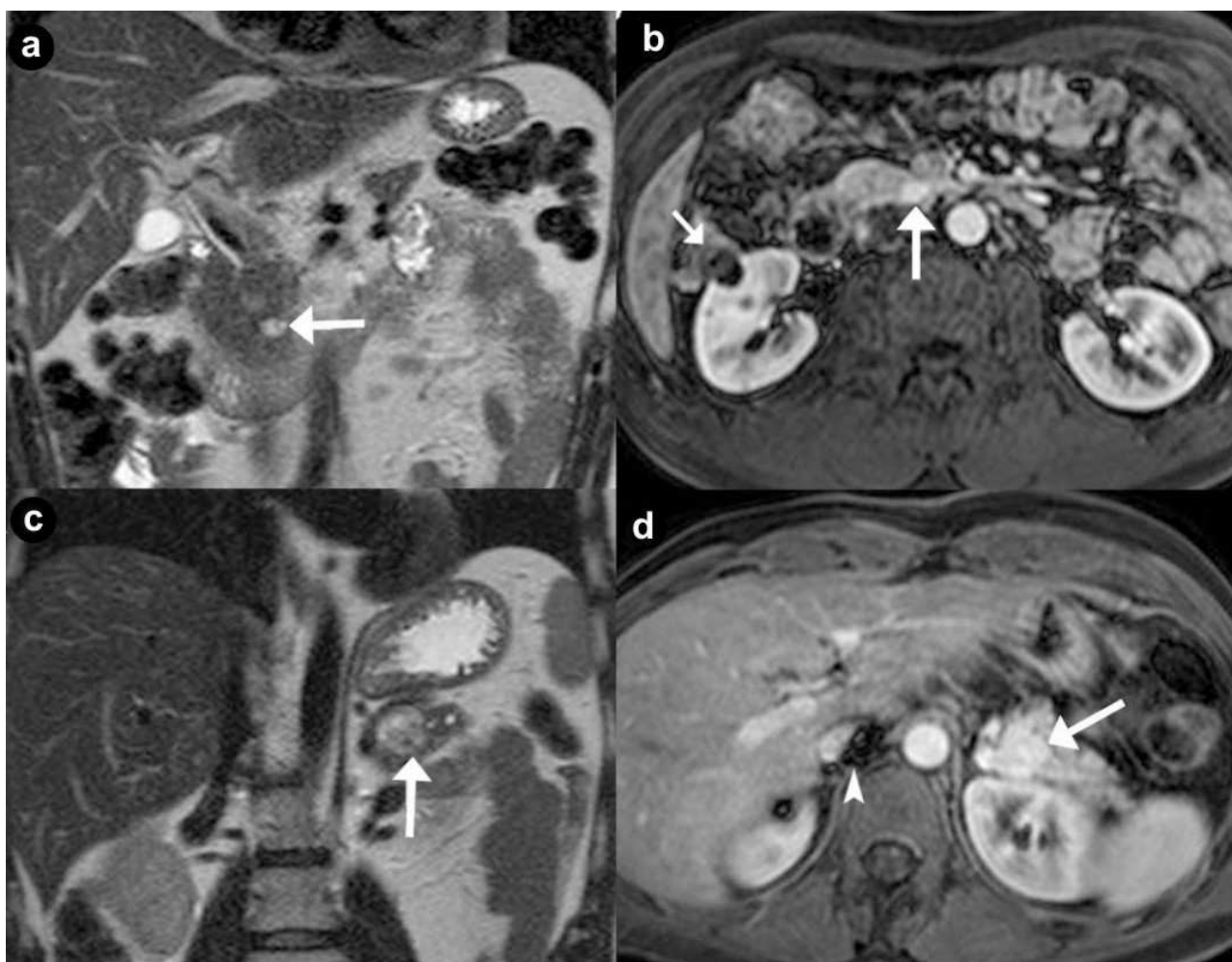
Figure 2. Pancreatic non functioning neuroendocrine tumors. Two cases suffering from VHL syndrome: a 39-year-old man (**a. b.**), and a 37-year-old man (**c. d.**). Coronal (**a. c.**) T2-weighted MR images; axial (**b. d.**) 3D volumetric gradient-echo T1-weighted fat suppressed images after intravenous contrast medium administration during arterial pancreatic phase of contrastographic dynamic study.

In pancreatic head, a small, nodular solid lesion with maximum diameter of 12 mm (**a. b.** arrow), hyperintense on T2-weighted MR images, with homogeneous enhancement after intravenous contrast medium administration during arterial pancreatic phase is present. Main pancreatic duct is normal and common bile duct is not dilated. Small complex cystic mass in the right kidney without enhancement after intravenous contrast medium administration (**b.**) is present (short arrow). In pancreatic body-tail a solid, round mass with maximum diameter of 23 mm (**c. d.** arrow), heterogeneously hyperintense on T2-weighted MR images, with homogeneous enhancement after intravenous contrast medium administration during arterial pancreatic phase, is present. Artifacts are recognizable in the site of right adrenal gland (arrowhead), due to the presence of metallic staples of previous adrenalectomy for pheochromocytoma.

1.000, respectively; and those of hypervascular solid neuroendocrine tumors were 1.000, 0.988, 0.986, and 0.878, respectively. The kappa values for vascular invasion and liver metastasis were 0.944 and 1.000, respectively.

Interobserver variability showed substantial agreement for the presence/absence (kappa=0.778) and site of pancreatic lesions in pancreatic head (kappa=0.712), in body-tail (kappa=0.770), and diffuse in all pancreatic gland of cystic non-functioning NET (kappa=0.690), as well as association of non-functioning NET and cystic lesions (kappa=0.730).

Interobserver variability showed almost perfect agreement for the following renal parameters: i) presence/absence; ii) unilateral/bilateral lesions, and iii) unique lesion/multiple lesions. Simple renal

cysts showed kappa values equal to 1.000, 0.988, and 1.000, respectively; complex renal cysts had values of 0.946, 0.956, 1.000, respectively; and solid hypovascular renal carcinomas values of 0.894, 0.902, 0.998, respectively. Renal vascular invasion showed perfect agreement (kappa=1.000).

Interobserver variability showed almost perfect agreement for all adrenal (kappa=0.978) and scrotal (kappa=1.000) parameters analyzed.

Interobserver variability showed substantial agreement for the presence/absence of retro-peritoneal lymph nodes (kappa=0.712).

In quantitative analysis, maximum diameter of single lesion or maximum diameter of major lesion in case of multiple lesions was 44.0 mm (mean value) in pancreatic unilocular fluid cystic lesions
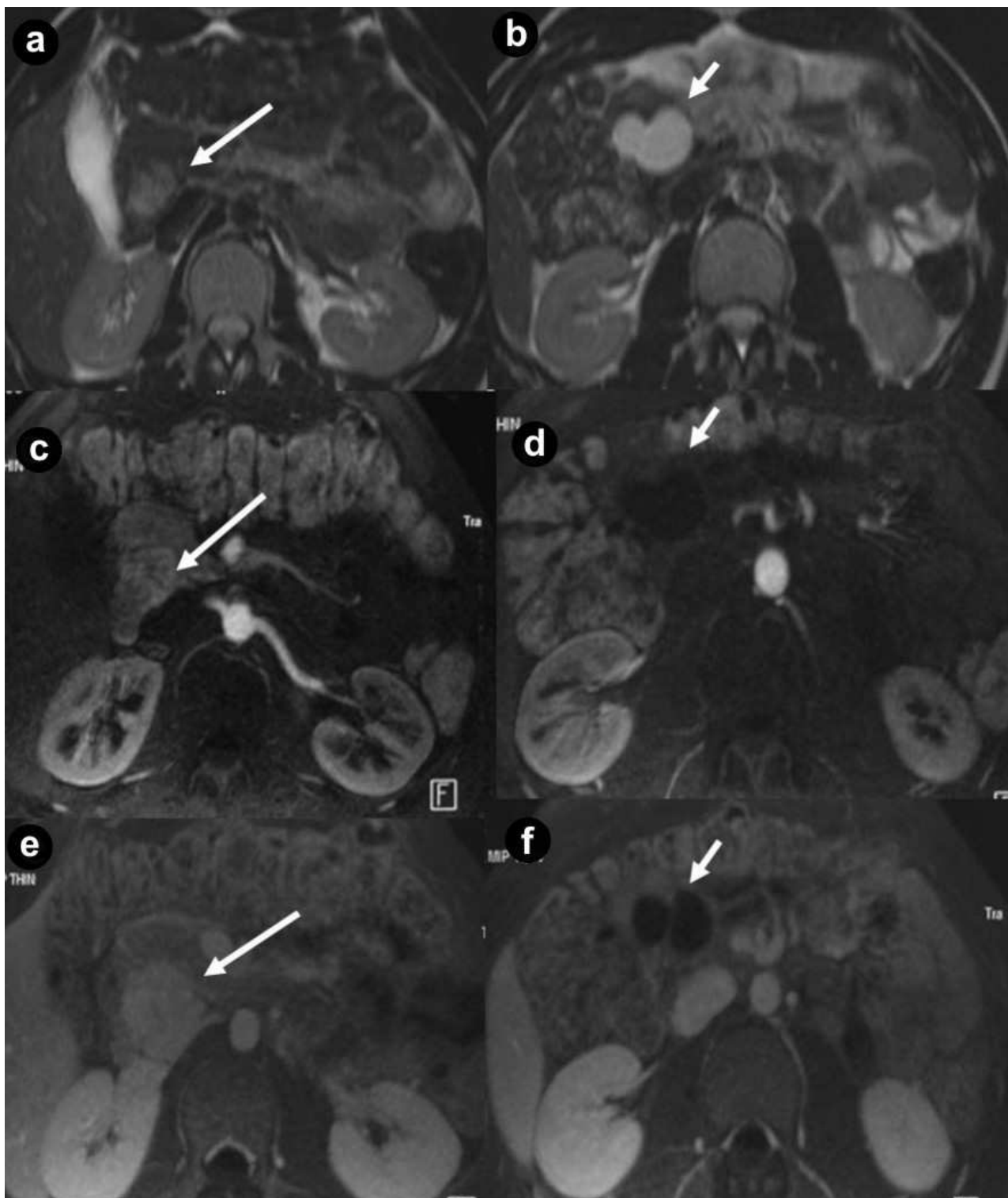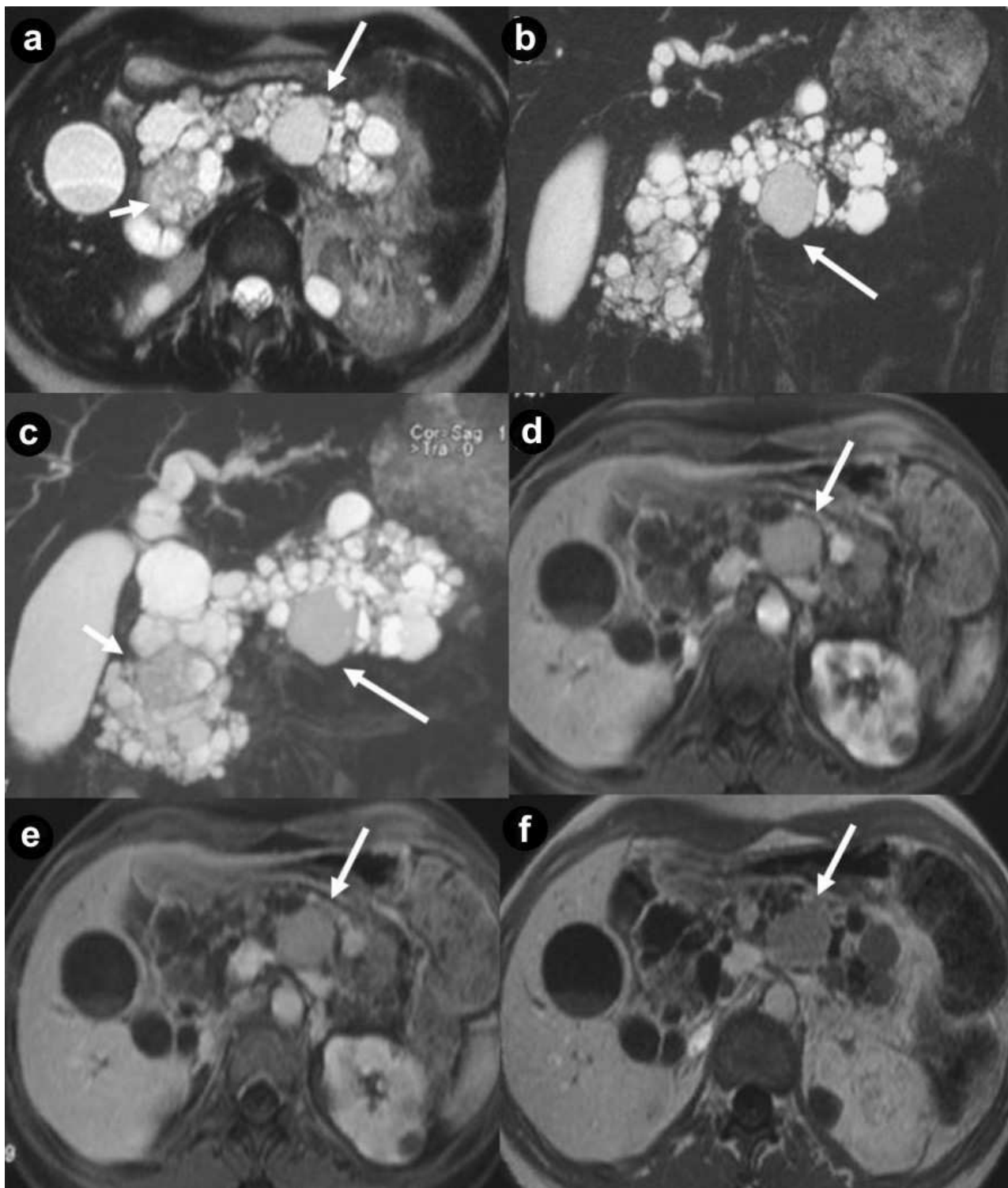
Figure 3. Pancreatic non functioning neuroendocrine tumor and pancreatic serous cystadenoma in the same patient: asymptomatic 24-year-old man. Axial (**a. b.**) T2-weighted MR images, axial 3D volumetric gradient-echo T1-weighted fat suppressed images after intravenous contrast medium administration during arterial pancreatic (**c. d.**) and portal venous (**e. f.**) phases of contrastographic dynamic study.
In pancreatic head a solid mass (**a.** arrow), heterogeneously hyperintense on T2-weighted MR images (**a.**) with homogeneous enhancement after intravenous contrast medium administration during arterial pancreatic phase of contrastographic dynamic study (**c.**), without wash-out in portal venous phase (**e.**) is present. In pancreatic head a cystic parenchymal lesion (short arrow), more hyperintense than solid mass, with fluid signal intensity on T2-weighted MR images (**b.**), without enhancement after intravenous contrast medium administration during arterial pancreatic (**d.**), and portal venous phases (**f.**), is visible. Inside the cystic lesion a septa is recognizable. Pancreaticoduodenectomy with Whipple procedure was performed. Histological specimen showed the presence of pancreatic macrocystic serous cystadenoma and non functioning neuroendocrine tumor of pancreatic head.
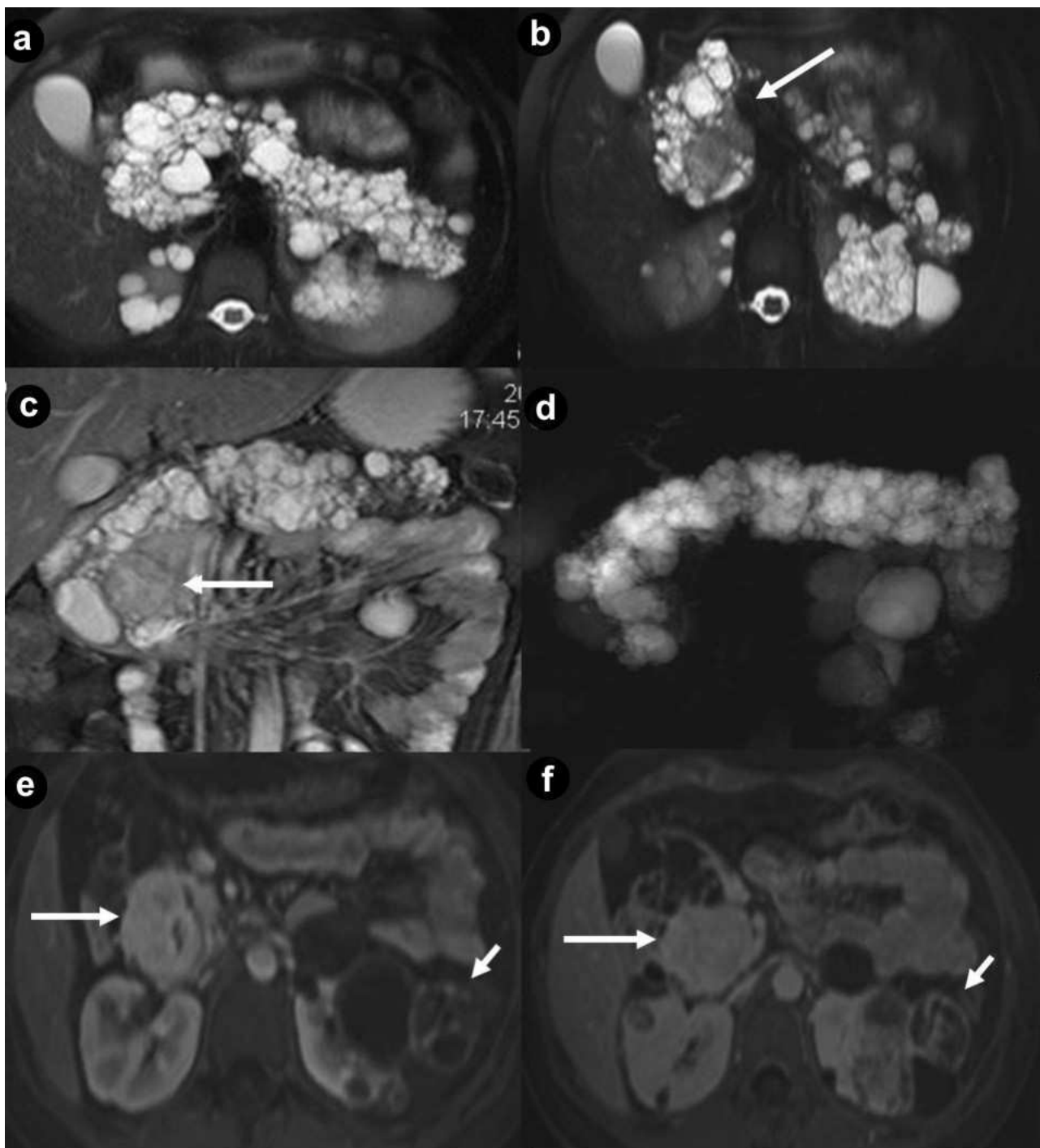
Figure 4. Pancreatic diffuse microcystic serous cystadenoma and pancreatic non functioning neuroendocrine tumor in the same patient. A 24-year-old woman with VHL disease and symptoms of pancreatic exocrine insufficiency. Axial (**a. b.**) and coronal (**c.**) T2-weighted MR images, MR cholangiopancreatography (**d.**) and axial 3D volumetric gradient-echo T1-weighted fat suppressed images after intravenous contrast medium administration during arterial pancreatic (**e.**) and portal venous (**f.**) phases of contrastographic dynamic study.

Pancreatic gland is enlarged and parenchyma is completely replaced by multiple, lobulated fluid cysts, hyperintense on T2-weighted MR images, with a "bunch of grapes" pattern (**a. b. c. d.**). In the pancreatic head, a round solid mass (arrow), with the signal intensity less high than other pancreatic cysts on T2-weighted MR images and homogeneous enhancement after intravenous contrast medium administration during arterial pancreatic phase (**e.**), with low wash-out in portal venous (**f.**) phase, is present. Multiple bilateral renal cystic lesions and large complex mass on the left kidney (short arrow), with fluid signal intensity, multiple solid septa and heterogeneous enhancement after intravenous contrast medium administration during arterial (**e.**) and portal venous (**f.**) phases, are detected.

Total pancreatectomy and surgical enucleation of the left renal mass were performed. Histological specimen showed the presence of pancreatic diffuse serous cystadenoma, non functioning neuroendocrine tumors of pancreatic head and cystic renal cell carcinoma of left kidney.

Figure 5. Pancreatic diffuse microcystic serous cystadenoma and pancreatic non functioning neuroendocrine tumor in the same patient. Asymptomatic 34-year-old woman, member of family affected to VHL disease. Axial (**a.**) and coronal (**b.**) T2-weighted MR images, MR cholangiopancreatography (**c.**) and axial 3D volumetric gradient-echo T1-weighted fat suppressed images after intravenous contrast medium administration during arterial pancreatic (**d.**), portal venous (**e.**) and delayed (**f.**) phases of contrastographic dynamic study.

Pancreatic gland is enlarged and parenchyma is completely replaced by multiple, lobulated fluid cysts, hyperintense on T2-weighted MR images, with a "bunch of grapes" pattern (**a. b. c.**). The wall of cystic lesions and septa inside them shows enhancement after intravenous contrast medium administration during arterial pancreatic (**d.**), portal venous (**e.**) and delayed (**f.**) phases. In pancreatic head and neck, some cysts result so small and so numerous as they show lower signal intensity on T2-weighted MR images compare to fluid lesions and appear at MR imaging like solid mass (short arrow). In the pancreatic body, a round solid mass (arrows), with the signal intensity less high than the other pancreatic cysts on T2-weighted MR images and homogeneous enhancement after intravenous contrast medium administration during arterial pancreatic phase (**d.**) with low wash-out during portal venous phase (**e.**) but hypointense on delayed (**f.**) phase, is present. Multiple bilateral renal fluid cysts are detected.

Splenopancreatectomy was performed. Histological specimen showed the presence of pancreatic diffuse serous cystadenoma and non functioning neuroendocrine tumors of pancreatic body-tail.
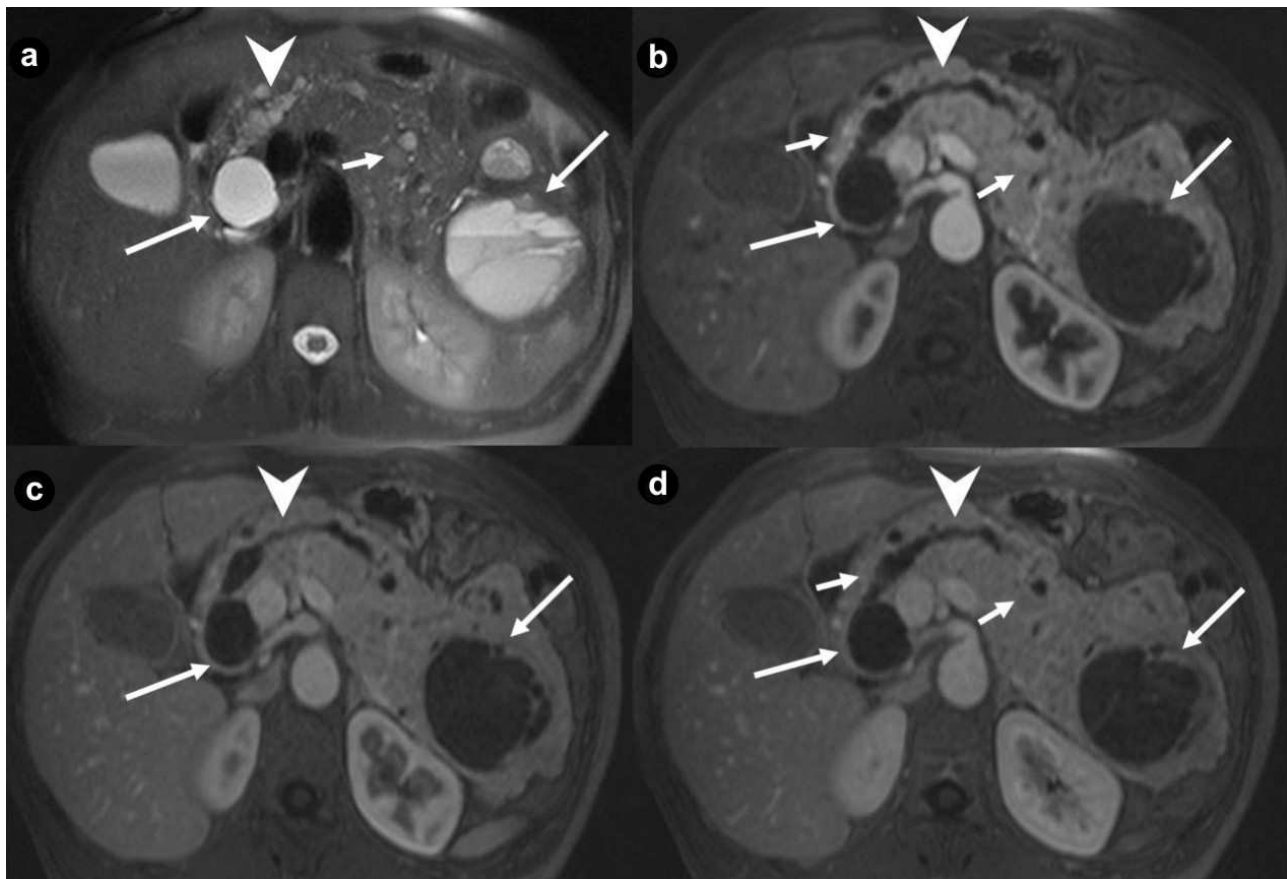
Figure 6. Pancreatic diffuse cystic non functioning neuroendocrine tumor. A 43-year-old woman affected by VHL disease. Axial T2-weighted MR images (**a.**) and 3D volumetric gradient-echo T1-weighted fat suppressed images after intravenous contrast medium administration during arterial pancreatic (**b.**), portal venous (**c.**) and delayed (**d.**) phases of contrastographic dynamic study.
Pancreatic gland is enlarged and parenchyma is thickened, completely replaced by multiple, lobulated fluid cysts, the largest in pancreatic head and tail (arrows), hyperintense in T2-weighted MR images, with thickened walls and irregular septa. Multiple small parenchymal nodules (small arrows), hyperintense on T2-weighted MR images but with lower signal intensity compared to fluid lesions, are visible in pancreatic body-tail and head. After intravenous contrast medium administration during arterial pancreatic (**b.**), portal venous (**c.**) and delayed phases (**d.**) walls and septa of cystic lesions show enhancement. Also multiple, small, solid parenchymal nodules enhance during pancreatic phase of dynamic MR study (short arrows). A large fluid cystic lesion in pancreatic head causes stenosis of main pancreatic duct and upstream duct dilatation (arrowhead).
Total pancreatectomy and retroperitoneal lymphadenectomy was performed. Histological specimen showed the presence of pancreatic diffuse non functioning neuroendocrine carcinoma with malignant cystic and solid lesions. Retroperitoneal adenopathy metastasis were present.

(range: 4-68 mm), 56.6 mm in serous cystadenomas (range: 21-98 mm), 42.0 mm in neuroendocrine solid tumors (range: 12-83 mm), 94 mm in cystic non-functioning NET (1 case of this tumor was only found), 50.5 mm in renal cysts (range: 4-80 mm), 60.0 mm in complex renal cysts (range: 10-90 mm), 32.4 mm in solid hypervascular renal carcinomas (range: 18-66 mm), 62.0 mm in adrenal solid hypervascular tumors (range; 32-84 mm), and 55.0 mm in scrotum fluid cystic lesion or cystadenoma.

DISCUSSION

Pancreatic Lesions

Pancreatic manifestations of VHL disease have different frequencies depending on the family group (0-77%) and consist of simple unilocular cystic lesions or simple pancreatic cysts, serous microcystic or micro/macro-cystic cystadenomas, neuroendocrine tumors (NET) and rarely adenocarcinoma [3, 4, 9, 15, 17].

Combined lesions occur, but the association of cystic lesions and neuroendocrine tumors is rare [3].

Simple Pancreatic Cysts or Unilocular Pancreatic Cystic Lesions

They are present at autopsy in 50-91% of patients with VHL disease [4, 17, 18, 19].

The pancreatic gland in patients with VHL disease may show a single or multiple unilocular cystic lesions, isolated, in groups or cluster. When multiple, the unilocular cystic lesions may substitute completely the gland [4, 9, 15, 17, 18, 19].

In our series unilocular pancreatic cystic lesions were present in 26.1% of patients with VHL disease (6 out of 23 patients).
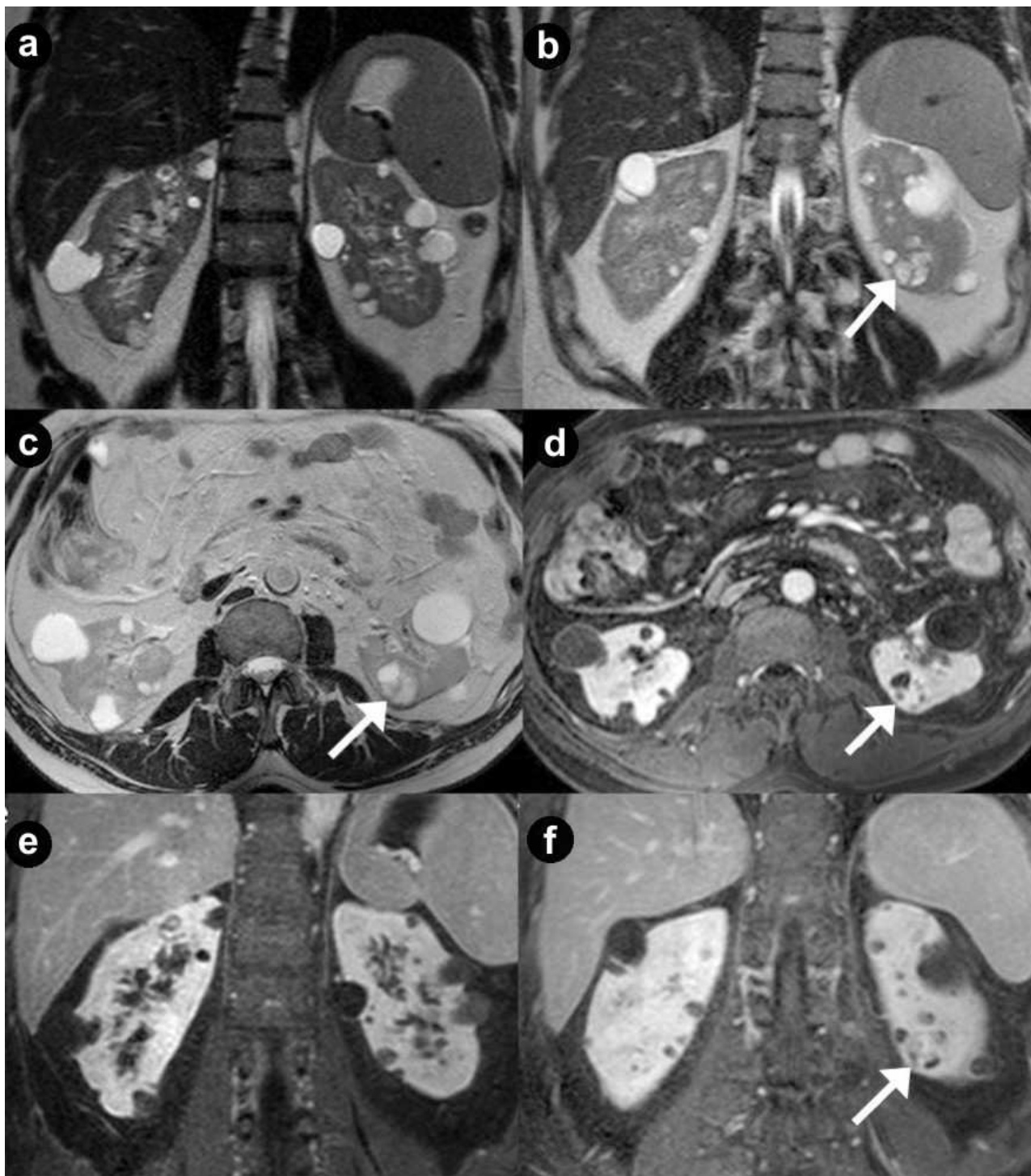
Figure 7. Renal cysts and cystic renal cell carcinoma. A 43-year-old man with VHL disease. Coronal (**a. b.**) and axial (**c.**) T2-weighted MR images; axial (**d.**) and coronal (**e. f.**) 3D volumetric gradient-echo T1-weighted fat suppressed images after intravenous contrast medium administration during arterial (**d. e.**) and venous (**f.**) phases of contrastographic dynamic study.
Multiple and bilateral simple, fluid renal cysts, with high signal intensity on the T2-weighted images (**a. b. c.**) and hypointense without enhancement after intravenous contrast medium administration during arterial (**d. e.**) and venous (**f.**) phases. In the lower pole of the left kidney a complex cystic mass (arrows) is present, with heterogeneous hyperintensity on the T2-weighted images, septa and solid areas enhanced after intravenous contrast medium administration during arterial (**d. e.**) and venous (**f.**) phases. Surgical enucleation of left renal lesion was performed. Histological specimen showed the presence of a cystic renal cell carcinoma.

To describe MR imaging findings of pancreatic lesions in VHL patients we needed pathological specimen and histological confirmation of MR imaging findings. So, symptomatic patients (13/23) were included in our retrospective evaluation; all of them were submitted to surgical procedure. On the other hand, we had no data of the pathological specimen of the remaining patients not submitted to pancreatic surgical procedure (10/23). This could explain the small frequency of unilocular
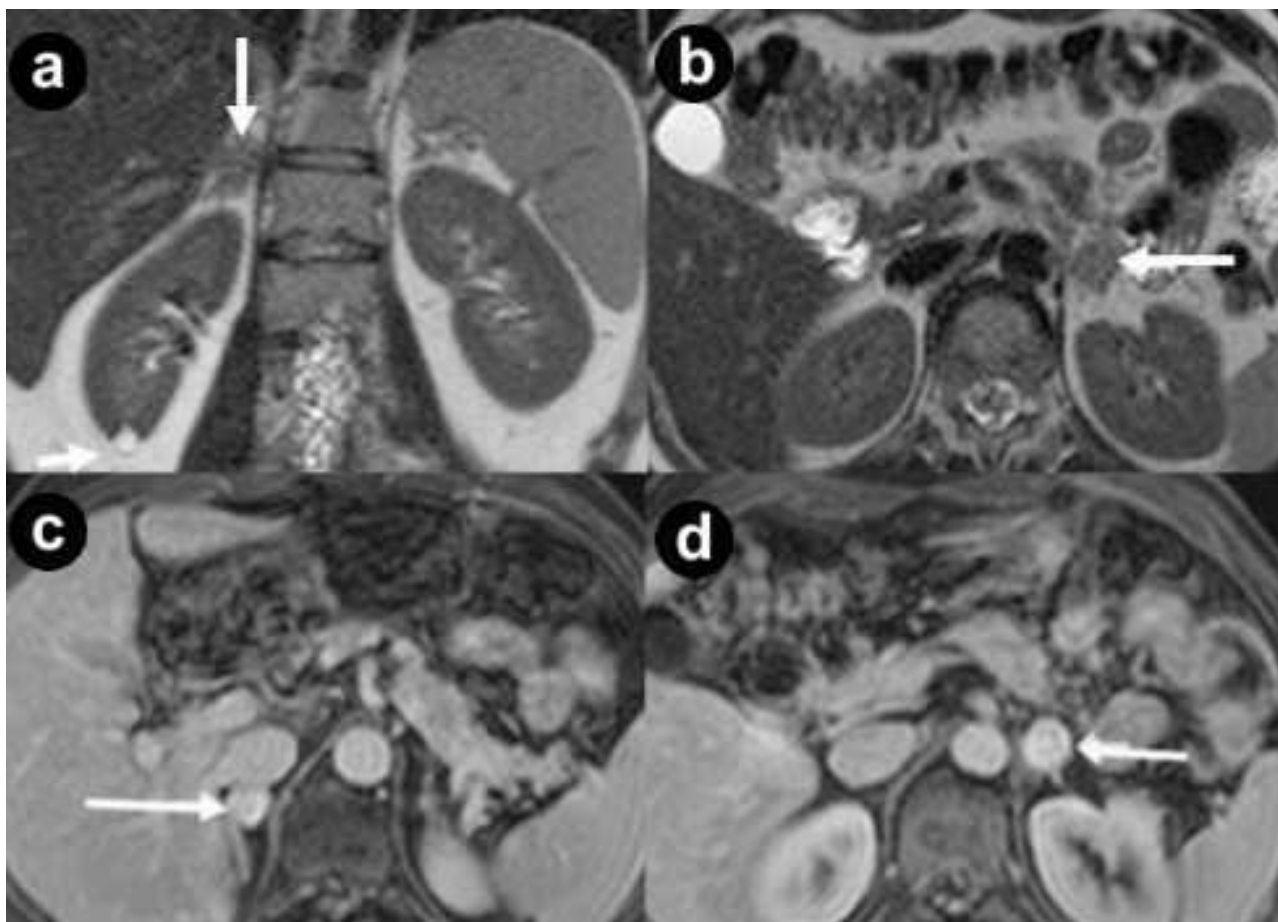
Figure 8. Adrenal pheochromocytomas. A 38-year-old man with VHL disease. Coronal (**a.**) and axial (**b.**) T2-weighted MR images; axial (**c. d.**) 3D volumetric gradient-echo T1-weighted fat suppressed images after intravenous contrast medium administration during portal venous phase of contrastographic dynamic study.
In both adrenal glands, small, round solid masses (arrows), with maximum diameter of 20 mm and intermediate signal intensity in T2-weighted MR images (**a. b.**) are present. The nodules show intense and homogeneous enhancement after intravenous contrast medium administration during dynamic study (**c. d.**). Small cyst at lower pole of right kidney (**a.** short arrow).
Bilateral open adrenalectomy was performed. Histological specimen showed the presence of adrenal bilateral pheochromocytomas.

cystic lesions observed in our series of VHL patients, when compared with other study cases [3, 9, 15, 17, 19, 20].

The average of maximum diameter of these cystic lesions was 44 mm (Figure 1abc).

These lesions are usually asymptomatic, but occasionally larger cysts may compress adjacent structures and cause symptoms. When symptoms are present, they frequently consist of minor abdominal discomfort, local pain, pancreatitis, obstructive jaundice and intestinal sub-occlusion [17, 18, 19, 20, 21]. Rarely, severe pancreatic cystic disease results in exocrine insufficiency requiring enzyme replacement [17, 18]. All our cases resulted asymptomatic.

At MR imaging [3, 9, 15, 16, 21] pancreatic cysts appear hypointense on T1-weighted images and hyperintense on T2-weighted images lesions (Figure 1ab), with no enhancement after intravenous gadolinium contrast medium administration (Figure 1c).

Pancreatic unilocular cystic lesions are extremely rare in the general population [20]. Therefore, the presence of a single cyst in a patient undergoing VHL disease screening because of a family history suggests a high probability of the disease.

Because frequently unilocular cystic pancreatic lesions in VHL disease are asymptomatic or associated with only mild symptoms, they are typically detected during screening examinations and may therefore facilitate the identification of gene carriers. In addition, pancreatic lesions may be the only abdominal manifestation and may precede any other manifestation by several years [17, 20]. So, imaging identification of these pancreatic lesions helps in earlier diagnosis of VHL disease.

Many studies have demonstrated the absence of significant progression of pancreatic cysts [15, 20] and therefore conservative management is recommended in these cases.

In presence of symptoms, aspiration of cystic content and injection of sclerosing substances may be performed [9].

Finally, it may be impossible to distinguish a cluster of benign unilocular cystic lesions from a serous microcystic cystadenoma. On the other hand, is also virtually impossible to distinguish a unique pancreatic cystic lesion from a unilocular serous cystadenoma in asymptomatic patients not submitted to surgical treatment. This can be another reason of the small frequency of unilocular cystic lesions and a high frequency of serous cystadenoma in our series of VHL patients.

In asymptomatic patients not submitted to surgical treatment, we considered serous microcystic cystadenoma a circumscribed, multilocular, hyperintense on T2-weighted MR sequence mass, with plurilobulated margins, thin walls, with multiple radially aligned thin septa, enhancing after intravenous gadolinium administration. On the contrary, we considered cluster of benign unilocular cystic lesions a group of hyperintense on T2-weighted MR sequence lesions, close to each other but separated, without septa and enhancing wall, and serous unilocular cystadenoma a circumscribed, hyperintense on T2-weighted MR sequence mass, with thin walls and one or rare thin septa inside fluid lesion.

Because of the benignity of both lesions, the presence of these lesions has no clinical implications [15, 20].

Figure 9. Papillary cystadenoma of the epididymis. A 35-year-old man with VHL disease. Coronal 3D volumetric gradient-echo T1-weighted fat suppressed images after intravenous contrast medium administration during portal venous phase of contrastographic dynamic study.
Bilateral complex cystic mass of epididymis with extratesticular site, fluid components, irregular septa inside the lesion and solid mural nodules which show enhancement after intravenous contrast medium administration during arterial phase (asterisks).
Testicular resection was performed. Histological specimen showed the presence of bilateral papillary cystadenoma of the epididymis.

Serous Cystadenomas

Serous cystadenoma have a lower incidence (approximately 12%) in VHL patients than pancreatic simple cysts [15, 17, 18, 19, 20, 21]. As the pancreatic simple cysts, serous cystadenomas are generally asymptomatic. Occasionally they may produce compressive symptoms and require surgical treatment [17, 18, 19].

In microcystic serous cystadenomas, MR images [3, 15, 16, 17] show a circumscribed, encapsulated mass, with plurilobulated margins and thin walls, hyperintense on T2-weighted (Figures 1de, 4abcd, and 5abc) and hypointense on T1-weighted images, with multiple and radially aligned thin septa, hypointense at T2-weighted images. A central fibrous scar with calcification is frequently present. Peripheral wall and septa enhance after intravenous gadolinium administration (Figure 1f, 5def). The septa are well depicted on T2-weighted MR images but the central scar is not. The use of a gradient-echo pulse sequence with a long echo time may bring out the susceptibility effects from the calcified scar. So, the fluid mass results composed of a grapelike cluster or "honeycomb pattern" of uniformly sized cysts with a diameter of 2 cm or smaller.

The small cysts are surrounded by large cysts in micro/macro-cystic serous cystadenoma.

In macrocystic serous cystadenoma, MR images identify a fluid lesion, unilocular or with one or rare thin septa inside lesion. The septa and thin peripheral wall of fluid lesion do not enhance after gadolinium-chelates injection during MR dynamic study (Figure 3bdf).

Magnetic resonance cholangiopancreatography (MRCP) is helpful in demonstrating the relationship of the mass to the main pancreatic duct. The main duct is almost never obstructed, but the duct and its branches may be marked or located.

Microcystic serous cystadenomas or micro/macro-cystic serous cystadenoma may be diffuse in all pancreatic gland [22, 23]. In this case the pancreas appears at MR imaging [23] markedly enlarged, with parenchyma almost completely replaced by innumerable cysts, with "bunch of grapes" pattern, present only in these patients (Figures 5 and 6).

In our series pancreatic serous cystadenomas were present at MR imaging in 47.8% of patients with VHL disease (Figures 1def, 3bdf, 4, and 5).

To obtain pathological specimen and histological confirmation of MR imaging findings we retrospectively evaluated symptomatic patients only (13 out of 23; all of them submitted to surgical procedure) and we do not know the pathological specimen of the remaining patients not submitted

to surgical procedure(10 out of 23). It can explain the high frequency of serous cystadenoma in our series of VHL patients, differently from other study cases. The average maximum diameter of these lesions was 56.6 mm and 34.8% of these cases were diffuse in all pancreatic gland (Figures 4 and 5); 8.7% were localized at pancreatic body-tail (Figure 1def) and 4.3% were localized at pancreatic head (Figure 3bdf). According to Agarwal *et al.* [22], in 13.0% of our cases, the serous cystadenoma (all of them diffuse in all pancreatic gland) were associated to hypervascular solid neuroendocrine tumors (Figures 4 and 5).

Neuroendocrine Tumors

The prevalence of NETs in VHL patients is reported to be about 5-17% [4, 9, 11, 15, 20, 21, 24, 25, 26, 27, 28, 29, 30].

In VHL patients these tumors are typically not functioning NET, asymptomatic, often slow growing lesions, and fewer than 10-30% of them metastasize [24, 25, 26, 27, 28, 29, 30, 31, 32]. Even when metastases occur, they are associated with relatively long survival times.

The NETs occur more frequently in VHL patients with pheochromocytoma and rarely are associated with pancreatic cystic lesions [4, 9, 15, 24].

Frequently NETs in VHL patients are smaller than 3.0 cm in diameter (Figure 2) and demonstrate slow growth rate [15, 24, 25, 26, 27, 28, 29, 30, 31, 32]. Indeed, almost 20% of lesions of 3.0 cm in diameter or larger had metastasized to the liver. Thus, while a majority of pancreatic NETs are small and benign, a minority can progress to metastatic disease. Active surveillance for these lesions is therefore justified [31, 32] and they may be observed rather than immediately removed. Therefore, their removal can be coordinated with surgery required for other lesions (pheochromocytomas or renal cancers), thus sparing the patient from undergoing multiple surgical procedures.

One-half of these lesions are reported to be located in the pancreatic head [24]. This suggest the possibility that the pancreatic head is predisposed to develop pancreatic NETs in patients with VHL disease. However, this hypothesis remains doubtful [9, 24].

At MR images [15, 24, 25, 26, 28, 29, 30, 33] these tumors are oval or round lesions, with well-demarcated margins, hypointense on the T1-weighted images, and show higher signal intensity than normal pancreatic parenchyma on T2-weighted images, but they have no so high signal intensity as cysts (Figures 2ac, 3a, 4bc, and 5bc).

They show intense and early enhancement after gadolinium-chelates injection during MR dynamic study, resulting hyperintense masses at enhanced pancreatic phase of MR study (Figures 2bd, 3c, 4e, and 5d), with a reduced or moderate reduced or non reduced signal intensity in successive venous and delayed phases of dynamic study because of wash-out, or low wash-out, or no wash-out of gadolinium contrast medium, respectively.

The smaller tumors enhanced homogeneously, while the larger tumors tend to enhance heterogeneously after contrast medium administration during the pancreatic arterial and portal venous phases on MR images. The vascular heterogeneity may be a sign of malignancy, since malignant lesions are often heterogeneous in vascular structure, perfusion, and vascular permeability [24, 25, 26, 27]. As tumors grow, the central portions become less vascularized, so necrotic areas and calcifications may compare [24, 25, 26].

More rarely than sporadic NETs, NETs in VHL patients are hypovascular lesions at MR images. They appear hypointense masses compared to surrounding parenchyma at MR enhanced pancreatic arterial phase.

Rarely NETs may be fluid lesions [34], hyperintense on T2-weighted MR images (Figure 6a). However, cystic lesions may be distinguished from cystic pancreatic NETs at imaging, since cystic pancreatic lesions show minimal thin peripheral enhancement, while cystic NETs demonstrated thick-walled enhancement (Figure 6bcd).

The identification of a hypervascular pancreatic mass in a patient with VHL is most likely indicative of the presence of a NET, much less likely indicative of pancreatic metastasis of renal adenocarcinoma or pancreatic hemangioblastoma, another possible but rare manifestation of VHL.

There is an association between pancreatic NETs and pheochromocytomas; in a retrospective study [24], 40% of patients had surgically confirmed adrenal pheochromocytomas.

High prevalence of pancreatic cystic disease in patients with VHL disease was also described in some studies. Approximately 60% of patients with VHL disease had moderate or severe cystic disease of the pancreas.

Thus, pancreatic NETs were usually found in patients with an otherwise normal pancreas or only mild pancreatic cystic disease.

In our series of VHL patients, solid pancreatic NETs were present in 34.8% of cases, all non functioning and hypervascular during enhanced pancreatic arterial phase of MR dynamic study (Figures 2, 3, 4, and 5). As mentioned above, to know pathological specimen and histological diagnosis in order to

confirm MR imaging findings, we included symptomatic patients only (13 out of 23) in our retrospective review, all of them submitted to surgical procedure. We do not know the pathological specimen of the remaining patients not submitted to surgical procedure(10 out of 23). This can explain the highest frequency of NETs in our series of VHL patients, compared to other study cases.

It also may be difficult to distinguish a unique pancreatic cystic lesion from cystic neuroendocrine non functioning tumor. This can be another reason of the small frequency of unilocular cystic lesions and a highest frequency of NETs in our series of VHL patients. We have considered as cystic non-functioning NET a cystic, fluid lesion with thickened enhanced walls and a simple cystic pancreatic lesion and a single fluid lesion without peripheral enhancement or showing minimal thin peripheral enhancement.

Differently to literature, in our series non functioning NETs had not a preferential site in pancreatic gland, resulting localized in 17.4% of cases in the pancreatic head (Figures 2ab, 3, and 4) and 17.4% in pancreatic body-tail (Figures 2cd and 5).

Only in 4.3% of our VHL cases, non-functioning NET was a cystic lesion, diffuse in all pancreatic gland (Figure 6), with fluid signal intensity and thickened walls enhancing during dynamic MR study.

In 17.4% of our series, we reported the association in the same patient of non-functioning NETs and pancreatic cystic lesions, many of them (3/23, 13.0%) were represented by diffuse serous cystadenomas (Figures 3, 4, and 5) and few of them (1/23, 4.3%) were represented by simple cysts.

In 8.7% of our VHL patients, all of them suffering from non-functioning NET, retroperitoneal lymph nodes metastasis were present and confirmed by pathological specimen.

In VHL patients of our series the mean value of maximum diameter of non-functioning NETs resulted 42 mm; vascular invasion and distant metastases were present in none patient.

Some authors recommend follow-up of these small lesions in VHL patients in order to check their development, or their conservative surgical treatment combined with other surgical abdominal procedures to be performed in these patients [24, 25, 26, 28, 29, 30, 31, 32, 33].

Pancreatic NETs in VHL patients are generally treated by using pancreas-sparing surgical procedures to minimize morbidity, including pancreatic exocrine and endocrine insufficiency. Lesions in the tail of the pancreas can be treated with distal pancreatectomy, whereas small lesions in the pancreatic head can be treated with enucleation.

Larger lesions require more aggressive surgery, including pancreaticoduodenectomy with Whipple procedure and total pancreatectomy [24, 25, 26, 28, 29, 30, 31, 32, 33, 35, 36].

In our VHL patients series of 23 patients, surgical treatment for non-functioning NETs was performed in 39.1% of cases (9 patients): pancreatico-duodenectomy with Whipple procedure in 13.0% (3 patients) (Figure 3), distal splenopancreatectomy in 13.0% (3 patients) (Figure 5), total pancreatectomy in 8.7% (2 patients) (Figures 4 and 6) and enucleation in 4.3% (1 patient).

No local and/or distant tumor recurrences are usually reported in radical surgery treatment of pancreatic neuroendocrine tumor in VHL patients, after a median time of five-year follow-up. Recently, a recurrence after a very long period of time was described [37], suggesting that a pancreatic neuroendocrine tumor associated with VHL syndrome may be more aggressive than that has previously been described, thus requiring a life-long follow-up.

Blansfield *et al.* [33] proposed three criteria to predict metastatic disease of pancreatic NET in patients with VHL disease: i) tumor size greater than or equal to 3 cm; ii) presence of a mutation in exon 3; and iii) tumor doubling time less than 500 days. If the patient has none of these criteria, they suggested that the likelihood of the patient's lesion resulting in metastatic disease is very low and the patient can be followed with a medical history, physical examination and radiologic surveillance (CT/MR follow-up) every 2-3 years. If one criterion is satisfied, the patient should be followed more closely by CT/MRI every 6 months to 1 year to detect the emergence of a second criterion. If 2 or 3 criteria are present, the patient should be considered for surgical management because of the great likelihood of future malignancy from pancreatic NET. The treatment strategy in patients with the metastatic disease is still controversial, depending on histological tumor types [25, 33, 35].

Renal Lesions

Renal Cysts

Renal cysts are present in 59-63% of patients with VHL disease [12]; more frequently they are multiple lesions and are reported bilateral in as many as 75% of patients [9, 12, 38, 39, 40]. They may vary from simple cysts, or fluid lesions with thin walls, without parietal enhancement after intravenous contrast medium administration at MR study, to complex cysts, with cystic and solid components, showing different macro- and microscopic

appearance and structure, until cystic renal cell carcinoma.

All these types of cystic lesions may occur in a single kidney.

In the epithelium lining the walls cyst, cells with clear cytoplasm are present [15, 19, 41, 42].

Many cysts are very small and not visible at imaging techniques because of their dimensions inferior to spatial resolution of imaging modalities [43]. The number and size of renal cysts are not correlated to lesion malignancy [3, 9, 15].

At MR imaging [3, 4, 9, 15, 16, 38, 39, 40] they result hypointense on T1-weighted images, and hyperintense on T2-weighted images (Figures 4ab, 5a, and 7abc), with no walls enhancement after intravenous gadolinium contrast medium administration (Figures 5def and 7def).

According to the literature, in our series simple renal cysts were present in 78.3% of patients. In 69.6% of our cases they were multiple and bilateral (Figures 4ab, 5, and 7).

Complex cysts were present in 56.5% of VHL patients (Figures 1a and 2b). The average maximum diameter of lesions was 50.5 mm in simple cysts and 60 mm in complex cysts.

Renal Carcinoma

Renal cell carcinoma occur in 28-45% of patients with VHL disease and it is a frequent cause of morbidity and mortality in these cases [3, 4, 9, 15]. The risk of renal cell carcinoma is much higher in these patients, with mutation of the VHL gene, than in the general population and the cancer occurs in younger VHL patients compared to cases of sporadic renal cell cancers (mean age: 30-36 years) [3, 9]. The most common histological type is clear cell carcinoma, which in VHL is frequently multicentric and bilateral [41, 42].

MR findings [3, 9, 15, 16, 38] of renal carcinoma in patients with VHL syndrome are low signal intensity at T1-weighted images and high signal intensity at T2-weighted images, hypervascular with enhancement during arterial phase of contrastographic dynamic study, hypointense with wash-out in venous phase solid mass. The hypervascularity of renal lesions is probably related to increased levels of vascular endothelial growth factors, and other angiogenic factors produced by these hereditary tumors [41, 42].

Frequently, renal carcinoma in patients with VHL syndrome may present as complex cystic masses [15, 19] with fluid component, mural nodules, thick walls and septa showing enhancement on T1-weighted images after intravenous gadolinium contrast medium administration (Figures 4ef and

7bcdef). Malignant complex cysts may show a low-signal intensity walls on T2-weighted images (pseudocapsule).

Frequently the whole range of different benign and malignant lesions is present in the same kidney (Figures 4 and 7).

According to the literature, in our series renal carcinoma or hypervascular solid masses were present in 47.8% of patients. They result multiple and bilateral in 45.5% of cases.

Cystic renal cells carcinoma or malignant complex cysts were present in 13.0% of VHL patients (Figures 4ef and 7bcdef).

It is reported that the risk of distant metastases of renal carcinomas with diameter less than 3 cm is low [44, 45].

The average maximum diameter of lesions in this series was 32.4 mm. Also in all our cases, liver metastases and retroperitoneal adenopathies were absent at the time of the diagnosis.

Both to save the renal function and to delay any future more aggressive treatment, the preferred treatment in renal cell carcinoma associated to VHL disease is nephron-sparing surgery due to the high probability of appearance of new renal neoplastic lesions. For this reason simple enucleation of the mass or partial nephrectomy are indicated [46].

In our series of 23 VHL patients, 14 cases (60.9%) underwent surgical treatment for malignant renal lesions: partial nephrectomy was performed in 8 cases (34.8%; Figures 4 and 7) and total nephrectomy in the remaining 6 patients (26.1%).

In patients with high surgical risk, in presence of small lesions (maximum diameter inferior to 3 cm), or in case of exophytic masses or of single tumor with maximum diameter between 3 and 5 cm, that would be difficult to remove with partial nephrectomy, it is possible to perform radio-frequency ablation [47]. Ablation is particularly suitable for patients with VHL disease because they have multiple renal cell carcinomas.

Early detection of renal carcinoma with screening enables such treatment rather than radical nephrectomy; furthermore, early treatment may prevent metastasis [38, 41, 42].

Pheochromocytomas

In the VHL patients pheochromocytomas arise only in presence of specific alleles of the VHL gene.

The frequency of this tumor varies therefore from 0% to 60% in different family groups [3, 11, 15, 48]. Two subtypes of VHL disease have been distinguished: the type 1, with no history of pheochromocytoma, and the type 2, with

pheochromocytoma history, in which pancreatic and renal cysts and tumors are very rare [9, 18].

In VHL patients, pheochromocytomas occur in younger age, they are more often bilateral (50-80%), multiple, ectopic and more rarely malignant than in sporadic cases [3, 4, 9, 15, 29].

Most tumors are localized in the adrenal glands, but 15-18% of the lesions are found in an extra-adrenal location (paragangliomas), in the retroperitoneal space near the origin of the superior mesenteric (organ of Zuckerkandl), at periaortic space, at perisplenic space, at intrarenal space, in the chest, in neck, and at skull base (glomus jugular and carotid body) [15, 49].

The ectopic pheochromocytomas (paragangliomas) are more common in VHL (15-18%) than in the general population [3].

The pheochromocytomas produce elevate level of catecholamines in the serum and urine and they can be symptomatic with hypertension, headaches, palpitations and flushing. In some cases of VHL syndrome, clinical symptoms of pheochromocytoma represent the onset of the disease and the tumor can be identified before the gene mutation.

However they may be asymptomatic, with negative laboratory tests and they may be discovered only occasionally or during the screening.

If an adrenal lesion is discovered at MDCT in VHL patient, MR is the imaging technique of choice because it is superior to MDCT in evaluating ectopic site of pheochromocytomas.

At MR imaging the lesions are usually iso- or hypointense on T1-weighted images compared to the liver, they do not lose signal intensity in T1-weighted images in opposition of phase, and they are hyperintense on T2-weighted images (Figure 8ac), with marked gadolinium enhancement [3, 4, 9, 15, 16, 50, 51, 52] during arterial phase of contrastographic dynamic study (Figure 8bd).

Atypical MR pattern are the low signal intensity on T2-weighted images and the presence of hemorrhagic areas [50].

A characteristic MR findings of paragangliomas may be the "salt and pepper" pattern, due to the presence of multiple serpentine and punctate areas of signal void variably distributed through the mass in all the MR sequences. They are believed to represent flow voids in the larger intratumoral vessels. [51].

The treatment of choice is still open adrenalectomy. However, it is possible to remove pheochromocytomas with laparoscopic partial adrenalectomy or enucleation, although the risk of recurrence is high [3, 15].

In our series pheochromocytomas resulted in 21.7% of VHL patients, with bilateral lesions in 17.4% of cases. Imaging diagnosis were confirmed by pathological specimen after open adrenalectomy in all cases.

Papillary Cystadenomas of the Epididymis

Cystadenoma of the epididymis is a rare epithelial tumor that originates from the Müllerian residual of connective tissue, with prominent papillae lined by glycogen-rich clear cells [53], similar to the appearance of serous cystadenoma of the ovary.

The tumor has no malignant potential. Therefore, no surgical treatment is required unless there is local pain [9].

In the general population the epididymal cystadenomas are extremely rare and always unilateral. The presence of bilateral cystadenomas of the epididymis is virtually pathognomonic of VHL [9, 54, 55]. The prevalence of papillary cystadenomas of the epididymis in male patients with VHL is about 1060% [9, 11].

The lesions, generally with a diameter of 2-3 cm, are most frequently localized in the head of the epididymis but may also involve the spermatic cord [9].

Patients suffering from cystadenoma of the epididymis may present a palpable scrotal hard mass, generally asymptomatic. Bilateral disease lead to infertility, due to obstructive azoospermia [9, 11].

Because these lesions are often palpable, imaging is not often required. Ultrasound is the diagnostic imaging method of choice for detection of scrotal lesions [56, 57]. MR imaging depicts a cystic mass with a high signal intensity on T2-weighted images, septa and/or mural solid nodules [58, 59]. The internal architecture of the lesion can be better demonstrated on gadolinium-enhanced T1-weighted imaging (Figure 9).

In our series we observed only one case of one epididymal papillary cystadenoma (4.3%), confirmed by pathological specimen after testicular resection (Figure 9).

CONCLUSIONS

Abdominal manifestations of VHL disease are different and protean. MR imaging plays an essential role in the identification of pancreatic and other abdominal lesions of VHL disease and their follow-up, in the screening of asymptomatic gene carriers, and in their long-term surveillance, to allow a more conservative therapeutic approach, and helps to improve the survival and quality of life.

Conflict of interest The authors have no potential conflict of interests

References

1. Richard S, Graff J, Lindau J, Resche F. Von Hippel - Lindau disease. Lancet 2004; 363:1231-4.

2. Maher ER. Von Hippel - Lindau disease. Curr Mol Med 2004;4:833-42.

3. Taouli B, Ghouadni M, Corre´as JM, et al. Spectrum of abdominal imaging findings in von Hippel-Lindau disease. AJR Am J Roentgenol 2003;181(4):1049-1054.

4. Hes FJ, Feldberg MA. Von Hippel-Lindau disease: strategies in early detection (renal-, adrenal-, pancreatic masses). Eur Radiol 1999;9(4): 598-610.

5. Banks RE, Tirukonda P, Taylor C, et al.Genetic and epigenetic analysis of von HippeleLindau (VHL) gene alterations and relationship with clinical variables in sporadic renal cancer. Cancer Res 2006;66:2000-11.

6. Maher ER, Iselius L, Yates JR, Littler M, Benjamin C, Harris R, Sampson J, Williams A, Ferguson-Smith MA, Morton N. Von Hippel-Lindau disease: a genetic study. J Med Genet 1991;28:443-447.

7. Seizinger BR, Rouleau GA, Ozelius LJ, et al. Von Hippel-Lindau disease maps to the region of chromosome 3 associated with renal cell carcinoma.Nature 1988;332(6161):268-269.

8. Latif F, Tory K, Gnarra J, et al. Identification of the von Hippel-Lindau disease tumor suppressor gene. Science 1993;260(5112):1317-1320.

9. Choyke PL, Glenn GM, Walther MM, et al. Von Hippel-Lindau disease: genetic, clinical, and imaging features. Radiology 1995;194(3):629-642.

10. Kaelin WG, Iliopoulos O, Lonergan KM, Ohh M. Functions of the von Hippel-Lindau tumour suppressor protein. J Intern Med 1995; 243:535-539.

11. Karsdorp N, Elderson A, Wittebol-Post D, et al. Von Hippel-Lindau disease: new strategies in early detection and treatment. Am J Med 1994;97(2): 158-168.

12. Melmon KL, Rosen SW. Lindau's disease: review of the literature and study of a large kindred. Am J Med1964;36:595-617.

13. Patard JJ, Rodriguez A, Rioux-Leclercq N, et al. Prognostic significance of the mode of detection in renal tumours. BJU Int 2002;90:358-63.

14. Friedrich CA.Von Hippel-Lindau syndrome: a pleomorphic condition. Cancer 1999;86(11 suppl):2478-2482.

15. Leung RS, Biswas SV, Duncan M, Rankin S. Imaging features of von Hippel-Lindau disease. Radiographics 2008; Jan-Feb 28(1):65-79.

16. Tattersall DJ, Moore NR. Von Hippel-Lindau disease: MRI of abdominal manifestations. Clin Radiol 2002;57:85-92.

17. Neumann HP, Dinkel E, Brambs H, et al. Pancreatic lesions in the von Hippel-Lindau syndrome. Gastroenterology 1991; 101(2): 465-471.

18. Maher ER, Yates JRW, Harries R, et al. Clinical features and natural history of von Hippel-Lindau disease. Q J Med 1990;77:1151-63.

19. Agrawal D, Maimone SS, Wong RC, Isenberg G, Faulx A, Chak A. Prevalence and clinical significance of pancreatic cysts associated with cysts in other organs. Dig Liver Dis 2011; Oct 43(10):797-801.

20. Hough DM, Stephens DH, Johnson CD, Binkovitz LA. Pancreatic lesions in von Hippel-Lindau disease: prevalence, clinical significance, and CT findings. AJR Am J Roentgenol 1994; 162(5): 1091-1094.

21. Torreggiani WC, Keogh C, Ismail KA, Munk PL, Nicolau S. Von Hippel-Lindau disease: a radiological essay. Clin Radiol 2002;57:670-680.

22. Agarwal N, Kumar S, Dass J, Arora VK, Rathi V. Diffuse pancreatic serous cystadenoma associated with neuroendocrine carcinoma: a case report and review of literature. JOP 2009; Jan 8 10(1):55-8. Review.

23. Kanno A, Satoh K, Hamada S, Hirota M, Masamune A, Motoi F, Egawa S, Unno M, Ishida K, Kimura K, Shuin T, Shimosegawa T. Serous cystic neoplasms of the whole pancreas in a patient with von Hippel-Lindau disease. Intern Med. 2011;50(12):1293-8.

24. Marcos HB, Libutti SK, Alexander HR, Lubensky IA, Bartlett DL, Walther MM. Neuroendocrine tumors of the pancreas in von Hippel-Lindau disease. Spectrum of appearances at CT and MR imaging with histopathologic comparison. Radiology 2002;225:751-758.

25. Tamura K, Nishimori I, Ito T, Yamasaki I, Igarashi H, Shuin T. Diagnosis and management of pancreatic neuroendocrine tumor in von Hippel-Lindau disease. World J Gastroenterol 2010; Sep 28 16(36):4515-8.

26. Binkovitz LA, Johnson CD, Stephens DH. Islet cell tumors in von Hippel-Lindau disease: increased prevalence and relationship to the multiple endocrine neoplasias. AJR Am J Roentgenol 1990; Sep 155(3):501-5.

27. Lubensky IA, Pack S, Ault D. et al. Multiple neuroendocrine tumors of the pancreas in von Hippel-Lindau disease patients: histopathological and molecular genetic analysis. Am J Pathol 1998;153:223-231.

28. Hammel PR, Vilgrain V, Terris B, Penfornis A, et al. Pancreatic involvement in von Hippel- Lindau disease. The Groupe Francophone d' etude de la Maladie de Von Hippel-Lindau.Gastroenterology 2000;119:1087-1095.

29. Delman KA, Shapiro SE, Jonasch EW, Lee JE, Curley SA, Evans DB, Perrier ND. Abdominal visceral lesions in von Hippel-Lindau disease: incidence and clinical behavior of pancreatic and adrenal lesions at a single center. World J Surg 2006; May 30(5):665-9.

30. Yamasaki I, Nishimori I, Ashida S, Kohsaki T. et al. Clinical characteristic of pancreatic neuroendocrine tumors in Japanese patients with von Hippel- Lindau disease. Pancreas 2006;33:382-385.

31. Libutti SK, Choyke PL, Alexander HR, et al. Clinical and genetic analysis of patients with pancreatic neuroendocrine tumors associated with von Hippel-Lindau disease. Surgery 2000;128:1022-1027.

32. Libutti SK, Choyke PL, Bartlett DL, et al. Pancreatic neuroendocrine tumors associated with von Hippel-Lindau disease: diagnostic and management recommendations. Surgery 1998;124:1153-1159.

33. Blansfield JA, Choyke L, Morita SY, Choyke PL, Pingpank JF, Alexander HR, Seidel G, Shutack Y, Yuldasheva N, Eugeni M, Bartlett DL, Glenn GM, Middelton L, Linehan WM, Libutti SK. Clinical, genetic and radiographic analysis of 108 patients with von Hippel-Lindau disease (VHL) manifested by pancreatic neuroendocrine neoplasms (PNETs). Surgery 2007;142(6):814-818;discussion 818.e1-2.

34. Neuzillet C, Vullierme MP, Couvelard A, Sauvanet A, Levy P, Richard S, Ruszniewski P, Hammel P. Difficult diagnosis of atypical cystic pancreatic lesions in von Hippel-Lindau disease. J Comput Assist Tomogr 2010;34(1):140-5.

35. Plöckinger U, Rindi G, Arnold R, Eriksson B, Krenning EP,de Herder WW, Goede A, Caplin M, Oberg K, Reubi JC,Nilsson O, Delle Fave G, Ruszniewski P, Ahlman H, Wiedenmann B. Guidelines for the diagnosis and treatment of neuroendocrine gastrointestinal tumours. A consensus statement on behalf of the European Neuroendocrine Tumour Society (ENETS). Neuroendocrinology 2004; 80:394-424.

36. Maeda H, Nishimori I, Okabayashi T Kohsaki T,et al.Total pancreatectomyfor multiple neuroendocrine tumors of the

pancreas in a patient with von Hippel-Lindau disease.Clin J Gastroenterol 2009;2:222-225.

37. Corleto VD, Cotesta D, Petramala L, Panzuto F, Pagnini C, Masoni L, Verrienti A, Delle Fave G, Filetti S, Letizia C. Late recurrence after surgical resection of a pancreatic tumor in von Hippel-Lindau disease. JOP 2009;4 10(5):562-5.

38. Meister M, Choyke P, Anderson C, Patel U. Radiological evaluation, management, and surveillance of renal masses in Von Hippel-Lindau disease. Clin Radiol 2009; Jun 64(6):589-600.

39. Choyke PL, Glenn GM, Walther MM, et al. The natural history of renal lesions in von Hippel-Lindau disease: a serial CT study in 28 patients. AJR Am J Roentgenol 1992;159(6):1229-1234.

40. Olea I, Vargas B, Sobrino B, Domínguez E. Abdominal manifestations in von Hippel-Lindau disease in a group of 7 patients and literature review. Radiologia 2009; Mar-Apr 51(2):198-203.

41. Choyke PL, Glenn GM, Walther MM, et al. Hereditary renal cancers. Radiology 2003;226:33-46.

42.Malek RS, Omess PJ, Benson RC Jr, Zincke H. Renal cell carcinoma in von Hippel-Lindau syndrome. Am J Med 1987;82(2):236-238.

43. Walther MM, Lubensky IA, Venzon D, et al. Prevalence of microscopic lesions in grossly normal renal parenchyma from patients with von Hippel-Lindau disease, sporadic renal cell carcinoma and no renal disease: clinical implications. J Urol 1995;154:2010-2014.

44. Ogawa O, Kakehi Y, Ogawa K, Koshiba M, Sugiyama T, Yoshida O. Allelic loss at chromosome 3p characterizes clear cell phenotype of renal cell carcinoma. Cancer Res 1991; 51:949-953.

45. Walther MM, Choyke PL, Glenn G, et al. Renal cancer in families with hereditary renal cancer: prospective analysis of a tumor size threshold for renal parenchymal sparing surgery. J Urol 1999; 161:1475-1479.

46. Herring JC, Enquist EG, Chernoff A, Linehan WM, Choyke PL, Walther MM, (2001) Parenchymal sparing surgery in patients with hereditary renal cell carcinoma: 10-year experience. J Urol,165:777-781.

47. Gervais DA, Arellano RS, Mueller PR. Percutaneous radiofrequency ablation of renal cell carcinoma. Eur Radiol 2001; 15(5): 960-967.

48. Choyke PL, Filling-Katz MR, Shawker TH, et al. Von Hippel-Lindau disease: radiologic screening for visceral manifestations. Radiology 1990;174: 815-820.

49. Rao AB, Koeller KK, Adair CF. From the archives of the AFIP. Paragangliomas of the head and neck: radiologic-pathologic correlation. Armed Forces Institute of Pathology. Radiographics 1999;19(6):1605-32.

50. Blake MA, Kalra MK, Maher MM. et al, (2004) Pheochromocytoma: An Imaging Chameleon. Radiographics,24:S87-S99.

51. Olsen WL, Dillon WP, Kelly WM, et al. MR imaging of paragangliomas. AJR 2004;148:201-204.

52. Lee KY, Oh YW, Noh HJ, et al. Extraadrenal Paragangliomas of the Body: Imaging Features. AJR 2006;187:492-504.

53 Woodward PJ, Schwab CM, Sesterhenn IA. From the archives of the AFIP: extratesticular scrotal masses: radiologic-pathologic correlation. Radiographics 2003;23(1):215-40. Review.

54. Smirnitopoulos JG, Lonergan GJ, Abbott RM. et al. Image interpretation Session: 1998. Radiographics 1999;19(1):205-233

55. Peyrì Reye E, Casalotos Serramia J. Cistoadenoma papilar de epidìdimo. Actas Urologicas Espanola 2000;761-763

56. Akbar SA, Sayyed TA, Jafri SZ, Hasteh F, Neill JS. Multimodality imaging of paratesticular neoplasms and their rare mimics. Radiographics 2003;23(6):1461-76.

57. Leung ML, Gooding GA, Williams RD. High-resolution sonography of scrotal contents in asymptomatic subjects. AJR Am J Roentgenol 1984;143(1):161-4.

58. Kim W, Rosen MA, Langer JE, Banner MP, Siegelman ES, Ramchandani P. US-MR Imaging correlation in pathologic conditions of the scrotum. Radiographics 2007;27(5):1239-53.

59. Funk KC, Heiken JP. Papillary Cystadenoma of the Broad Ligament in a Patient with von Hippel-Lindau Disease. AJR 1989; 153:527-528.